





Critical patch size reduction by heterogeneous diffusionM. A. F. dos Santos ¹, V. Dornelas ^{1,2}, E. H. Colombo ^{3,4} and C. Anteneodo ^{1,5}¹*Department of Physics, PUC-Rio, Rua Marquês de São Vicente 225, 22451-900, Rio de Janeiro, RJ, Brazil*²*ICTP-SAIIR & IFT-UNESP, Rua Dr. Bento Teobaldo Ferraz 271, 01140-070, São Paulo, SP, Brazil*³*Department of Ecology & Evolutionary Biology, Princeton University, Princeton, New Jersey 08544, USA*⁴*Department of Ecology, Evolution, and Natural Resources, Rutgers University, New Brunswick, New Jersey 08901, USA*⁵*Institute of Science and Technology for Complex Systems (INCT-SC), Rio de Janeiro, Brazil*

(Received 6 August 2020; revised 6 October 2020; accepted 13 October 2020; published 29 October 2020)

Population survival depends on a large set of factors and on how they are distributed in space. Due to landscape heterogeneity, species can occupy particular regions that provide the ideal scenario for development, working as a refuge from harmful environmental conditions. Survival occurs if population growth overcomes the losses caused by adventurous individuals that cross the patch edge. In this work, we consider a single species dynamics in a patch with a space-dependent diffusion coefficient. We show analytically, within the Stratonovich framework, that heterogeneous diffusion reduces the minimal patch size for population survival when contrasted with the homogeneous case with the same average diffusivity. Furthermore, this result is robust regardless of the particular choice of the diffusion coefficient profile. We also discuss how this picture changes beyond the Stratonovich framework. Particularly, the Itô case, which is nonanticipative, can promote the opposite effect, while Hänggi-Klimontovich interpretation reinforces the reduction effect.

DOI: [10.1103/PhysRevE.102.042139](https://doi.org/10.1103/PhysRevE.102.042139)**I. INTRODUCTION**

Species typically experience a patchy landscape, where only within certain regions individuals can find resources, shelter, and other key ingredients for survival [1]. The landscape spatial structure shapes diverse macroscopic ecological patterns, affecting, for instance, the stability and diversity of ecosystems [2,3]. Particularly, the fragmentation and degradation of the habitats, accelerated by human activities, have been producing significant impacts on ecosystems, leading many species to extinction [4,5]. Thus, it is, more than ever, a matter of interest to understand the role that habitat spatial features exert on species survival.

Focusing on a single patch, a central problem is to determine the critical patch size for species survival. Typically, there exists a minimum size L_c that separates the extinction and survival regimes. Then, if the patch size L is bigger than L_c , the population can grow, achieving a stationary profile at long time, while it goes extinct otherwise. The specific value of L_c depends on the details of the environment and population dynamics.

Pioneer investigations have addressed species survival assuming a time-independent bounded habitat and that individuals diffuse and reproduce with constant rates [6–8]. More recently, theoretical developments have been made to include demographic fluctuations, which arise from the stochastic character of the birth-death process [9], and experimental realization using specific strains of bacteria was performed to check the validity of the theory [10]. Beyond this classical case, previous works have discussed the effect of the spatiotemporal structure of the environment [11–15], advection [16,17], chemotaxis [18], and nonlinear response [19]. These

features can affect the value of L_c , as they substantially modify the flux of individuals through the habitat edge [20,21]. Furthermore, it has been shown that the common sense that larger patches favor species survival breaks down if a strong nonlinearity is present [19]. Similarly, in the multispecies context, it has been shown that small patches can have high conservation value [22,23].

Despite previous works have already tackled the critical patch size problem from many different perspectives, the effect of the space-dependent diffusion coefficient has not been sufficiently addressed. Several mechanisms can make the diffusion coefficient depend on the particular location inside the patch. For instance, the composition and structure of the medium through which individuals move can change, facilitating, or hindering, their mobility. This is characteristic of transition zones (ecotones) between habitat and nonhabitat regions which can distort animal movement [24,25]. Also, behavioral responses can affect mobility, as when individuals perceive at a distance [26] the drastic change in the environmental conditions near the edge of the habitat [21,27–30]. Regardless of the mechanisms that regulate the spatially dependent diffusion coefficient, heterogeneity would affect the residence time of the organisms in the patch [31], thus impacting the critical patch size.

The role of space-dependent diffusion on the critical patch size has been studied before in simplified settings, assuming an abrupt change close to the edge of the patch [32,33]. In this work, we extend this investigation for the case where the diffusion coefficient within the patch has a general form.

We consider a single species that grows and moves in a bounded domain, with diffusivity that varies in space. At the

microscopic level, each individual performs a random walk that in the overdamped limit, in one dimension, is described by

$$\dot{x} = \sqrt{2D(x)} \eta(t), \quad (1)$$

where $x(t)$ is the position of the walker at time t , D is the spatially varying diffusion coefficient, and η is a zero-mean noise. Equation (1) constitutes a minimal model for environment-dependent mobility, assuming that the perception is local and individuals are memoryless. Thus, we are neglecting directional movement that can arise when individuals take decisions either by integrating information over long distances [26,34] or by using memory, as in the case of chemotaxis [35,36].

Animal tracking data from bacteria to mammals [37–40] reveal that movement fluctuations, represented by η in Eq. (1), have a probability density function that can range from Gaussian to heavy tailed depending on the species and environmental conditions. Furthermore, temporal correlations are ubiquitous in the trajectories of the organisms, introduced by their behavior or by the environment (e.g., plankton in a turbulent flow [37]). For the sake of mathematical tractability of the problem, without disregarding the biological origins of the noise in Eq. (1), we first assume that η is a zero-mean Gaussian noise with arbitrarily small (but non-null) correlation time. Independently of how the correlation decays in time, the limit of small correlation time leads us to the Stratonovich perspective of Eq. (1), where η is now a Gaussian white noise [41,42]. The corresponding equation for the diffusion process in terms of the population density $\rho(x, t)$ is given by $\partial_t \rho = \partial_x \sqrt{D(x)} \partial_x \sqrt{D(x)} \rho$, which has been derived and studied in the literature [43–47].

To complete the continuous-field description, accounting for the birth-death process, we include a term $f(\rho)$, which is only required to admit a Taylor expansion around the null population state. Then, the evolution equation for our problem reads as

$$\frac{\partial}{\partial t} \rho(x, t) = \frac{\partial}{\partial x} \sqrt{D(x)} \frac{\partial}{\partial x} \sqrt{D(x)} \rho(x, t) + f(\rho(x, t)), \quad (2)$$

with $x \in [-L/2, L/2]$, where L is the size of the patch, and subject to Dirichlet bound boundary conditions. The zero-density boundary condition $\rho(x = \pm L/2, t) = 0$ mimics the harmful effects of the surroundings, which impose strong death rates, immediately killing the individuals that leave the patch. Although apparently drastic, this simplification has been useful in the context of homogeneous diffusion, and allows a first approach to the problem.

In Sec. II we derive an analytical expression to predict the critical patch size for the problem described by Eq. (2) and provide illustrative examples for specific forms of $D(x)$. By comparing these results with the scenario in which the diffusion coefficient takes the average value inside the patch, $\bar{D} = \frac{1}{L} \int_{-L/2}^{L/2} D(x) dx$, we show that heterogeneous diffusion has a nontrivial effect on population survival. We demonstrate that, under the Stratonovich interpretation, heterogeneous diffusion promotes the reduction of the critical patch size when contrasted to the averaged case, where $D(x) = \bar{D}$. Moreover, this holds for any kind of diffusivity profile within the patch. For particular cases, including the stochastic, rectangular,

sinusoidal, and power-law diffusivity profiles, we provide the explicit expression for the critical patch size. A mechanistic perspective on how heterogeneous diffusion can emerge due to behavioral responses to the patch edge is also presented. At last, we discuss in detail the influence of the different stochastic interpretations of Eq. (1) and their applicability, in Sec. III. Section IV contains final remarks about the result.

II. CRITICAL PATCH SIZE UNDER SPACE-DEPENDENT DIFFUSION

The standard approach to obtain the critical patch size is based on the linear stability of the dynamics close to the extinction state $\rho(x, t) = 0$. In this regime, we Taylor expand the growth term in Eq. (2) up to first order. Noting that $f(0) = 0$, the remaining term is given by $f(\rho) \simeq r\rho$, where $r = f'(0)$. Then, Eq. (2) becomes

$$\frac{\partial}{\partial t} \rho(x, t) = \frac{\partial}{\partial x} \sqrt{D(x)} \frac{\partial}{\partial x} \sqrt{D(x)} \rho(x, t) + r\rho(x, t), \quad (3)$$

where $x \in [-L/2, L/2]$, with absorbing boundaries.

To circumvent the spatial dependency on D , we define [48]

$$y(x) = \int^x dx' \frac{1}{\sqrt{D(x')}}, \quad (4)$$

which allows us to rewrite Eq. (3) as

$$\frac{\partial}{\partial t} \bar{\rho}(y, t) = \frac{\partial^2}{\partial y^2} \bar{\rho}(y, t) + r\bar{\rho}(y, t), \quad (5)$$

where $\bar{\rho}(y, t) = \sqrt{D(x)} \rho(x, t)$, and the new absorbing boundary condition is $\bar{\rho}(y(\pm L/2), t) = 0$. Thus, in the new variable y , the problem reduces to that of the homogeneous diffusion treated in classical works [6–8,49], where individuals perform a standard state-independent Brownian motion.

The population survives in the long time if the extinction state is unstable, and the initial condition is non-null. Solving Eq. (5) by the method of separation of variables or through Fourier series, the contribution of each mode is $\bar{\rho}_n(y, t) = e^{\lambda_n t} \cos(n\pi y/Y)$, where $Y = y(L/2) - y(-L/2)$ and $\lambda_n = r - (n\pi/Y)^2$, with $n = 1, 2, \dots$. The population will grow in time if there is at least one mode n with $\lambda_n > 0$. Noting that λ_1 is the maximal rate, then it is clear that the condition for population survival is given by $\lambda_1 > 0$. Otherwise, all other modes have negative growth rate. Therefore, the critical condition $\lambda_1 = 0$ leads to

$$Y_c = \int_{-L_c/2}^{L_c/2} \frac{1}{\sqrt{D(x)}} dx = \frac{\pi}{\sqrt{r}}. \quad (6)$$

For a homogeneous environment with constant $D(x) = \bar{D}$, the known expression $\tilde{L}_c \equiv \pi \sqrt{\frac{\bar{D}}{r}}$ is recovered [49]. The critical patch size arises from the balance between the flux that crosses the boundary and the growth inside the patch, as a consequence, it increases with \bar{D} but decreases with r .

For the general heterogeneous case, let us consider the discretized version of the integral in Eq. (6), i.e., $Y_c \simeq \frac{L_c}{N} \sum_{i=1}^N [D(x_i)]^{-1/2}$. First notice that Y_c remains the same by shuffling the values of $D(x_i)$ within the integration interval. In other words, different profiles with the same distribution of values (see example in Fig. 1) yield the same result in Eq. (6).

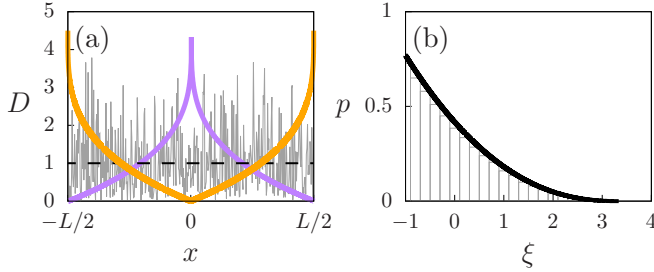


FIG. 1. Diffusion coefficient profile and corresponding distribution. (a) Diffusion coefficient (purple solid line) for a power-law profile, Eq. (15) with $\alpha = 0.3$, and its rearranged versions: mirrored halves (orange solid line) and randomly shuffled (gray solid line). The dashed horizontal line highlights the average level. (b) Distribution of the deviation from the average $p(\xi)$, which is the same in both cases, thus generating identical result in Eq. (6). Gray bars are from the numerical shuffling of $D(x)$ and the solid line the analytical result obtained from Eq. (11) (see Sec. IID).

Mathematically, this is due to the fact that the integrand is a function of $D(x)$ only, which is a consequence of the linearity of the birth-death process contemplated in Eq. (3).

Furthermore, it is useful to write $D(x) = \bar{D}[1 + \xi(x)]$, such that $\langle \xi \rangle = 0$ and $\xi > -1$ for the positivity of D , putting into evidence the variations ξ around a reference level. We use this form into the discretized version of Eq. (6), namely,

$$\frac{L_c}{N} \sum_{i=1}^N (1 + \xi_i)^{-1/2} \simeq \tilde{L}_c, \tag{7}$$

and search the extreme values of $h(\{\xi_i\}) = \sum_{i=1}^N (1 + \xi_i)^{-1/2}/N$, under the constraint $g(\{\xi_i\}) = \sum_{i=1}^N \xi_i/N = 0$. Through the method of Lagrange multipliers, we impose $\partial_{\xi_i}(g - \lambda h) = 0$, obtaining $\xi_i = 0$ for all i . From the analysis of the bordered Hessian, this corresponds to a minimum, with value $h = 1$. Then, from Eq. (7), in the continuum limit ($N \rightarrow \infty$), we get $L_c < \tilde{L}_c$.

Therefore, heterogeneous diffusion has the remarkable feature of typically producing a critical patch size smaller than in the corresponding averaged case, as we will see in the examples discussed in the following sections.

Noting that the distribution of the values of the diffusion coefficient is the key feature, we focus on heterogeneities with distribution preserved under changes of the size L . In terms of $D(x)$, this happens when the diffusivity depends on the position through the scaling x/L , that is $D(x) = \bar{D}[1 + \xi(2x/L)]$. In this case, Eq. (6) becomes

$$L_c = \frac{\tilde{L}_c}{\frac{1}{2} \int_{-1}^1 [1 + \xi(z)]^{-1/2} dz} \leq \tilde{L}_c. \tag{8}$$

Performing a power-series expansion of the integrand around $\xi = 0$, and taking into consideration that $\langle \xi \rangle = \int_{-1}^1 \xi(z) dz = 0$, at the lowest order, we obtain

$$L_c = \frac{\tilde{L}_c}{1 + \frac{3}{16} \int_{-1}^1 [\xi(z)]^2 dz} \leq \tilde{L}_c, \tag{9}$$

with equality holding in the case of homogeneous diffusion, which clearly indicates that, for small variations, the critical patch size is smaller than that produced by the homogeneous environment with the same average diffusivity, and this deviation increases with the variability of D .

A. Stochastic perspective

Since the main object that characterizes the heterogeneity and determines the value of the critical patch is the distribution $p(\xi)$, it is natural to develop a stochastic view of the diffusion profile, instead of thinking about the shape of $D(x)$. The following results provide a connection between these two perspectives, which will help to understand the particular cases tackled next.

We can interpret the deviation ξ as a stochastic variable that assumes values in the interval $(-1, \infty)$ with a certain probability density function (PDF) $p(\xi)$, which must verify $\langle \xi \rangle = \int_{-1}^{\infty} \xi p(\xi) d\xi = 0$. Following this idea, Eq. (8) can be rewritten as

$$L_c = \frac{\tilde{L}_c}{\int_{-1}^{\infty} [1 + \xi]^{-1/2} p(\xi) d\xi}, \tag{10}$$

allowing us to discuss the impact of heterogeneity in terms of the PDF $p(\xi)$.

This PDF can be obtained from a given profile of the diffusivity. In fact, $\xi = D(z)/\bar{D} - 1 \equiv \phi(z)$, where $z = 2x/L$ can be interpreted as a random variable that is uniform in the interval $[-1, 1]$, i.e., its PDF is $q(z) = \frac{1}{2}$ for $|z| \leq 1$. Then, $p(\xi)$ is obtained from $q(z)$, through a change of variables, namely,

$$p(\xi) = \frac{1}{2} \sum_{i=1}^{N(\xi)} |d\phi_i^{-1}(\xi)/d\xi|, \tag{11}$$

where the index i counts, for each value of ξ , the $N(\xi)$ solutions of $\phi(z) = \xi$, where the derivatives are computed.

B. Rectangular profile

Perhaps the simplest nonhomogeneous case occurs when $D(x)$ assumes two values inside the patch of size L instead of the single one in the homogeneous case. Let us say a region of length $\beta L < L$ with coefficient $D_0(1 + d)$, while the coefficient is D_0 otherwise, as illustrated in Fig. 2(a). It can be defined through the Heaviside step function H as

$$D(x) = D_0 \left[1 + d H \left(\beta - \frac{2|x|}{L} \right) \right], \tag{12}$$

where D_0 is related to the mean value through $\bar{D} = D_0(1 + d\beta)$, $0 < \beta < 1$ and $d\beta > -1$ for positivity. The associated PDF is $p(\xi) = [1 - \beta]\delta(\xi + \frac{d\beta}{1+d\beta}) + \beta\delta(\xi - \frac{d(1-\beta)}{1+d\beta})$, a sum of two Dirac delta functions [see Fig. 2(b)].

From Eq. (8), we obtain the explicit expression for the critical size [see Fig. 2(c)]

$$L_c/\tilde{L}_c = \frac{\sqrt{1+d}}{\sqrt{1+\beta d}[(1-\beta)\sqrt{1+d} + \beta]} \leq 1. \tag{13}$$

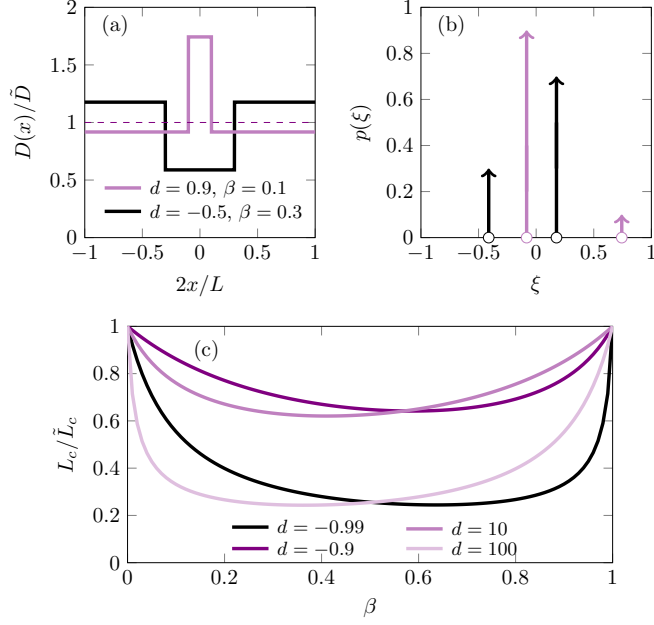


FIG. 2. Rectangular. Space-dependent diffusion coefficient scaled by its mean value $D(x)/\bar{D} = 1 + \xi$ (a), probability density function $p(\xi)$ (b), critical patch size ratio L_c/\tilde{L}_c vs β (c), given by Eq. (13), such that βL is the width of the central nucleus. In (b) the arrows represent Dirac delta functions.

It does not depend on the localization of the nucleus, which can be shifted from the origin, or even fragmented in many nuclei, of total size βL . It only depends on the proportion of the patch β adopting either of the two values.

When $d \rightarrow -1$, the denominator of Eq. (6) diverges, such that L_c must vanish. Conversely, in the opposite limit, when $d \rightarrow \infty$, L_c diverges. The homogeneous case occurs when $d = 0$, or $\beta = 0$ or 1 , and it requires the maximal patch size for survival. Moreover, we can see in Fig. 2(c) that there is an optimal value of β that minimizes L_c/\tilde{L}_c . Also note the high contrast between heterogeneous and homogeneous diffusion, when $d \gg 1$ or $d \simeq -1$, yielding a reduction of 75% of the critical size in the cases shown.

C. Sinusoidal profile

Another important case is when the variation around the mean value of the diffusion coefficient is sinusoidal [Fig. 3(a)], that is

$$D(x) = D_0 \left[1 + a \cos \left(\frac{2k\pi x}{L} + \phi \right) \right]. \quad (14)$$

When an integer number of periods fits the patch (i.e., $k \in \mathbb{Z}$), $\bar{D} = D_0$, and the result for the ratio L_c/\tilde{L}_c depends neither on the phase constant ϕ nor in the periodicity given by k , because the distribution of values remains unchanged. In fact, Eq. (11) yields $p(\xi) = 1/(\pi\sqrt{a^2 - \xi^2})$ for $|\xi| < a < 1$, which only depends on the amplitude a [see Fig. 3(b)]. Differently, when k is noninteger, $\bar{D} = D_0[1 + a \cos \phi \sin(k\pi)/(k\pi)]$ and the ratio of critical sizes depends on k as well as on the phase ϕ [see Fig. 3(c)]. In particular, for integer k and small amplitude, Eq. (9) predicts $L_c/\tilde{L}_c \simeq 1/[1 + (3/16)a^2]$.

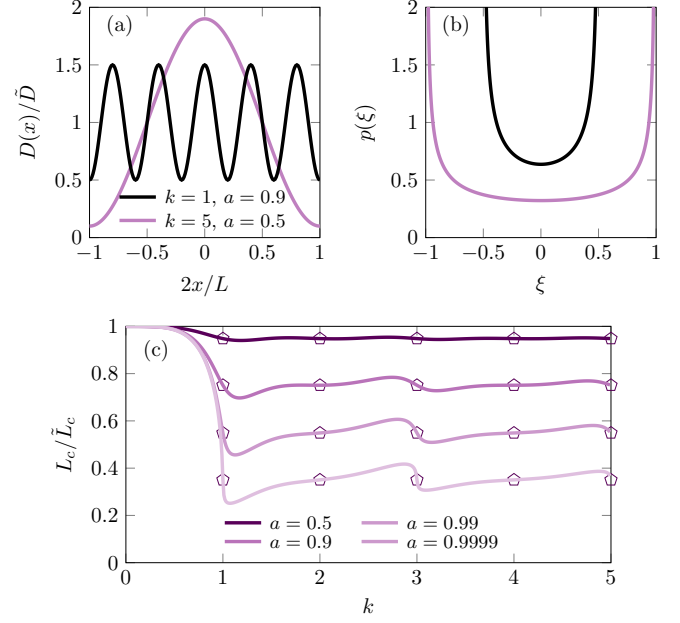


FIG. 3. Sinusoidal. Same as in Fig. 2 for the sinusoidal diffusivity, with $\phi = 0$. In (b), the PDF corresponds to any integer k . In (c) the symbols highlight that the critical ratio remains invariant for integer values of k , even if it were $\phi \neq 0$.

D. Power-law profile

Let us consider the *power-law* function

$$D(x) = D_0 \left(1 - d \left| \frac{2x}{L} \right|^\alpha \right), \quad (15)$$

where $D_0 = \bar{D}(\alpha + 1)/(\alpha + 1 - d)$. It leads to the ratio of critical sizes

$$L_c/\tilde{L}_c = \left[\sqrt{1 - \frac{d}{\alpha + 1}} {}_2F_1 \left(\frac{1}{2}, \frac{1}{\alpha}, 1 + \frac{1}{\alpha}, d \right) \right]^{-1} \leq 1, \quad (16)$$

which goes to one in the limit $\alpha \rightarrow \infty$.

For the particular case $d = 1$, $D(x)$ vanishes at the boundaries. In this case, $\xi(z) = [1 - (\alpha + 1)|z|^\alpha]/\alpha$, with probability $p(\xi) = (1 - \alpha\xi)^{1/\alpha - 1}/(\alpha + 1)^{1/\alpha}$ in $[-1, 1/\alpha]$. When $\alpha = 1$ (triangular profile), it corresponds to the uniform distribution in $[-1, 1]$. The limit $\alpha \rightarrow 0$ yields the anomalous case $D(x) = -\bar{D} \ln |2x/L|$, corresponding to the exponential $p(\xi) = \exp(-\xi - 1)$. However, for $d \neq 1$, in the limit $\alpha \rightarrow 0$, we also recover the homogeneous case, as in the limit $\alpha \rightarrow \infty$. In Fig. 4, we plot the ratio of critical sizes vs α , for a concave power-law profile $d = 0.96 > 0$ (solid line).

E. Edge-response profile

When modeling the mechanisms responsible for triggering the spatial dependency on individuals' mobility, the scaling dependence [i.e., $D(x) = D(x/L)$] might not be suitable. In these cases, the use of the explicit expression (8) becomes compromised. But, note that, directly from Eq. (6), we can address a much broader scenario. Then, to spark possible ideas in this sense, let us discuss the case where mobility is a function of the distance from the patch edge. This can

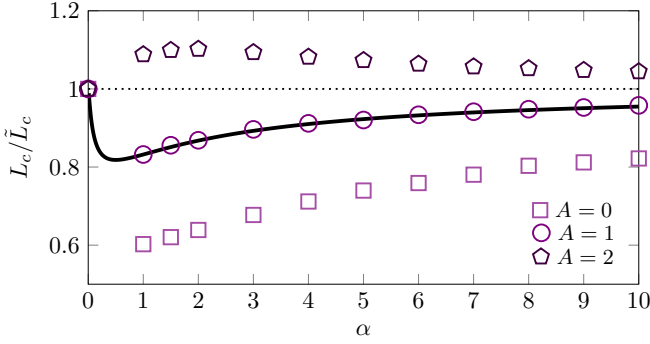


FIG. 4. Critical size ratio for the power-law case defined in Eq. (15), with $d = 0.96$ (solid line), following Eq. (16). Symbols correspond to numerical simulations for different values of the prescription parameter A , defined in Eq. (17), which will be introduced later in Sec. III. In the limits $\alpha \rightarrow 0$ and $\alpha \rightarrow \infty$, we have $\tilde{L}_c/L_c \rightarrow 1$ in all cases because $D(x) \rightarrow \bar{D}$. The horizontal dotted line highlights the unity ratio.

reflect changes in the landscape structure and composition during the transition from the habitat and nonhabitat regions known as *ecotone*. Alternatively, it can mimic the behavioral changes when individuals perceive the patch boundary (e.g., by sensing signals released by the patch [26]).

Assuming that individuals' mobility is reduced near the boundary, independently of the mechanisms behind this response, the diffusion coefficient takes the form of $D(x) = D_0[1 - \gamma(|x - L/2|)]$ where γ is a function verifying $\gamma(0) = 1$ and vanishing far from the boundary, such that the diffusion coefficient attains its maximum value D_0 .

A simple case that suits this scenario is given by $D(x) = D_0\{1 - \exp[-(|x| - L/2)/\ell]\}$, where ℓ is the characteristic scale of the response to the edge. This diffusive profile is depicted in Fig. 5(a) and the critical patch size as a function of the response scale ℓ in Fig. 5(b). Note that the profile shape is not preserved as the patch size increases [Fig. 5(a)]. Hence, Eq. (8) cannot be applied, but Eq. (6) yields the closed form $L_c = 4\ell \ln\{\cosh[\pi\sqrt{D_0/r}/(4\ell)]\}$ [Fig. 5(b)]. In the limit $\ell \rightarrow 0$, the profile converges to the homogeneous case, which produces $L_c = \tilde{L}_c$. As ℓ increases, L_c decreases, vanishing at

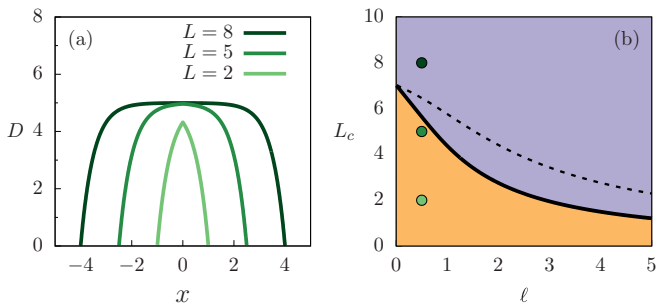


FIG. 5. Diffusion coefficient (a) and critical patch size (b) for an edge distance-dependent mechanism with the form $D(x) = D_0\{1 - \exp[-(|x| - L/2)/\ell]\}$ with $D_0 = 5.0$ and $\ell = 0.5$. In (b), for $r = 1$, the orange and lilac regions correspond to the extinction and survival phases, respectively. The dashed line represents \tilde{L}_c . Greenish circles correspond to the cases in (a).

$\ell \rightarrow \infty$. In the examples of Fig. 5(a) (with $\ell = 0.5$), $L_c \simeq 5.64$, as a consequence, for $L = 2$ and 5 , the population goes extinct, while for $L = 8$ it survives, as indicated by the dots with correspondent colors in Fig. 5(b). Although the critical patch size for the average value of D , \tilde{L}_c , has no closed form, we numerically checked that the statement $L/\tilde{L}_c \leq 1$ remains valid [dotted line in Fig. 5(b)].

III. OTHER INTERPRETATIONS OF THE SPACE-DEPENDENT DIFFUSION

The derivation of the macroscopic term for the diffusion processes from the stochastic individual level is not unique. There are different versions of a space-dependent diffusion equation [43,50–53] and all of these forms converge to the standard case when the diffusion coefficient is a constant in space and time. For all versions, the probability density $\rho(x, t)$ depends on the particular form of $D(x)$. A general class of heterogeneous-diffusion equations is

$$\frac{\partial}{\partial t} \rho(x, t) = \frac{\partial}{\partial x} \left\{ D(x)^{1-\frac{A}{2}} \frac{\partial}{\partial x} [D(x)^{\frac{A}{2}} \rho(x, t)] \right\}, \quad (17)$$

in which A is, in principle, a positive real number ($A = 1$ in our case). For $A \in \{0, 1, 2\}$, it defines the heterogeneous diffusion equation accordingly to different well-known prescriptions: Hänggi-Klimontovich ($A = 0$), Stratonovich ($A = 1$), and Itô ($A = 2$) formalisms. A possible underlying stochastic dynamics associated to Eq. (17) is given by Eq. (1), with η being a zero-mean Gaussian white noise, accompanied by the interpretation associated to the value of A . Alternatively, we can adopt, for instance, the Stratonovich prescription, and modify the stochastic equation adding a drift term associated to the chosen value of A , yielding $\dot{x} = (1 - A)D'(x)/2 + \sqrt{2D(x)}\eta(t)$.

This general form can be used to access the consequences of each interpretation in relevant macroscopic outcomes. For instance, recently, the general class of diffusive process in Eq. (17) has been used to investigate the impact of each prescription in the normalization of the probability distribution of a particle diffusing in a heterogeneous environment with $D(x) \propto |x|^\beta$ [54]. In this section, we address the role of the different interpretations of Eq. (1) on the critical patch size.

Rather than entering the interpretation dilemma, it may be more valuable to understand the origins and dynamics responsible for the noise in question, which will naturally lead to the appropriate interpretation. In our case, we have adopted the Stratonovich interpretation ($A = 1$), as mentioned in the Introduction, implicitly assuming that the noise η in Eq. (1) has a vanishing temporal correlation but still much longer than the relaxation time promoted by the inertia of the particles (individuals) [55]. Note that this consideration precedes Eq. (1), for which the overdamped limit has already been taken. More generally, depending on the microscopic details of the walk performed by the individuals, different values of A , even fractional ones [56], might be appropriate. For instance, when the particle dynamics relaxation time and the noise temporal correlation vanish, with the former surpassing the latter one, the Itô interpretation ($A = 2$) is the one that naturally emerges [55].

In Fig. 4, we compare the outcomes for different values of A . In order to do this, we numerically integrated Eq. (2) using the generalized diffusion term in Eq. (17) starting from the null homogeneous state plus a positive small random noise. We applied a standard forward-time-centered-space scheme which is fourth-order Runge-Kutta in time and second order in space, with discrete-time step $\Delta t = 10^{-5}$ and cell size $\Delta x = 0.01$.

We observe that the ratio L_c/\tilde{L}_c has significantly different values that increase with A . These results can be understood in light of results on the mean first passage time under heterogeneous diffusion. To do that, first recall that the critical patch size is achieved from the balance between diffusive losses at the borders and growth in the habitat. In other words, this occurs when the individuals' habitat residence time τ_h equals the reproduction interevent time τ_r , i.e., individuals reproduce exactly once before hitting the boundary and dying. For the homogeneous diffusion case, in which all interpretations produce identical values, $\tau_h \sim L^2/D$ and $\tau_r \sim 1/r$, which leads to $L_c \sim \sqrt{D/r}$ [10]. Under heterogeneous diffusion, it has been shown that τ_h is significantly affected by A [31]. In the case discussed here, τ_h increases with A , leading to a larger critical patch size as A increases. This picture, however, can change depending on the particular problem treated [31].

Lastly, note the result obtained from Eq. (7), that $L_c/\tilde{L}_c \leq 1$ for any $D(x)$, was derived for the diffusion equation associated to $A = 1$ and it is not expected to apply for any A . In fact, for the Itô case, $A = 2$, in Fig. 4, $L_c/\tilde{L}_c > 1$.

IV. FINAL REMARKS

We have shown that space-dependent diffusion, which appears as prescribed by Stratonovich interpretation, typically favors survival by reducing the critical patch size in the population dynamics described by Eq. (3).

We noted that Eq. (6) is not affected by shuffling the values of $D(x)$, which allowed the analysis from the perspective of the distribution of values around the mean $p(\xi)$. However, it is important to comment that the presence of any correlation between population growth and diffusion, such as a density-dependent diffusion coefficient [19], would change the form of Eq. (6) in such a way that the specific location and values of D would matter.

Assuming that the type of heterogeneity present, characterized by $p(\xi)$, is kept invariant, we investigated the cases in which the profile of the diffusion coefficient scales with the habitat size. This allowed us to extract simple expressions to show how heterogeneous diffusion affects the critical habitat size in comparison to the average level. We also provided an illustration of the nonscaling case, which similarly reduces the critical size, in accord with Eq. (7).

Furthermore, despite we argue that the Stratonovich interpretation is the suitable one for our biological context, we also discuss the impact of other interpretations in our results. In the studied case of Fig 4, we observed that, while Stratonovich ($A = 1$) interpretation reduces the critical patch size, the Hänggi-Klimontovich ($A = 0$) interpretation reinforces that effect. That is, the more anticipative is the noise,

the stronger is the reduction. Contrarily, the Itô ($A = 2$) prescription, which is nonanticipative, promotes the opposite effect.

All of these results highlight that the details of how individual behavior and spatial structure of the environment change inside patch boundaries should be taken into account in ecological management and natural reserve (refuge) design [32]. This adds to the point that neglecting the internal variability can lead to incorrect predictions about the macroscopic behavior of the system, a fact that has already been remarked in other ecological contexts [57,58].

The extent of the validity of our results may be limited by some simplifications in our model. In this paragraph, we discuss their possible impact and realistic features that would be worth to include in future extensions of our work. (i) In the present model, we adopted a continuous-field description of the population dynamics which neglects the stochasticity inherent to the birth-death processes. This is reasonable when the density of particles is large, which is more common in microorganisms' population [10]. In cases where the density is low, stochastic fluctuations dominate the dynamics leading to population extinction in finite time, regardless of the patch size [9,28]. Nevertheless, previous results show that the critical size L_c given by Eq. (2) with $D(x) = D_0$ remains a good indicator for the separation between the regimes of short and long extinction times [9]. (ii) With regard to dimensionality, it would be interesting to extend our study, performed for one-dimensional settings, particularly for two dimensions. Recent studies on the individual's residence time in higher dimensions [31,59,60] might provide useful tools to overcome the analytical challenges involved in this task. (iii) The discrepancy between the results under Stratonovich and Itô interpretations suggest that temporal correlations may play a crucial role, then it would be interesting to address our problem in the presence of different types of colored noise. (iv) A density-dependent growth, e.g., with a power-law dependence which is nonlinearizable [19], or with a birth-death process which is also spatially dependent [30] would break down the shuffling statement (Fig. 1) bringing the shape of the profile to the spotlight. (v) Finally, let us comment that alternatively to our partial differential equation approach, it would be interesting to perform agent-based simulations of a finite population [61,62]. This may help to address the impact, on the critical habitat size, of dimensionality, correlations, and other realistic features of the behavior at the individual level [36].

ACKNOWLEDGMENTS

We thank R. O. Vallejos for helpful suggestions. M.A.F.S., V.D., and C.A. acknowledge partial financial support by the Coordenação de Aperfeiçoamento de Pessoal de Nível Superior-Brazil (CAPES)-Finance Code 001. C.A. also acknowledges partial support by Conselho Nacional de Desenvolvimento Científico e Tecnológico (CNPq) and Fundação de Amparo à Pesquisa do Rio de Janeiro (FAPERJ). V.D. also acknowledges partial support by FAPESP through the ICTP-SAIFR Grant No. 2016/01343-7 and postdoctoral Fellowship No. 2020/04751-4.

- [1] M. G. Turner, R. H. Gardner, and R. V. O'Neill, *Landscape Ecology in Theory and Practice: Pattern and Process* (Springer, New York, 2001).
- [2] I. Hanski, *Metapopulation Ecology*, Oxford Series in Ecology and Evolution (Oxford University Press, New York, 1999).
- [3] L. Fahrig, *Annu. Rev. Ecol. Evolution Systematics* **34**, 487 (2003).
- [4] S. L. Maxwell, R. A. Fuller, T. M. Brooks, and J. E. M. Watson, *Nat. News* **536**, 143 (2016).
- [5] J. D. Congdon, A. E. Dunham, and R. C. Van Loben Sels, *Conserv. Biol.* **7**, 826 (1993).
- [6] H. Kierstead and L. B. Slobodkin, *J. Mar. Res.* **12**, 141 (1953).
- [7] J. G. Skellam, *Biometrika* **38**, 196 (1951).
- [8] D. Ludwig, D. G. Aronson, and H. F. Weinberger, *J. Math. Biol.* **8**, 217 (1979).
- [9] S. Berti, M. Cencini, D. Vergni, and A. Vulpiani, *Phys. Rev. E* **92**, 012722 (2015).
- [10] N. Perry, *J. R. Soc. Interface* **2**, 379 (2005).
- [11] R. S. Cantrell and C. Cosner, *J. Theor. Biol.* **209**, 161 (2001).
- [12] T. Neicu, A. Pradhan, D. A. Larochelle, and A. Kudrolli, *Phys. Rev. E* **62**, 1059 (2000).
- [13] A. L. Lin, B. A. Mann, G. Torres-Oviedo, B. Lincoln, J. Käs, and H. L. Swinney, *Biophys. J.* **87**, 75 (2004).
- [14] M. Ballard, V. M. Kenkre, and M. N. Kuperman, *Phys. Rev. E* **70**, 031912 (2004).
- [15] E. H. Colombo and C. Anteneodo, *Phys. Rev. E* **94**, 042413 (2016).
- [16] E. Pachepsky, F. Lutscher, R. M. Nisbet, and M. A. Lewis, *Theor. Pop. Biol.* **67**, 61 (2005).
- [17] A. B. Ryabov and B. Blasius, *Math. Model. Nat. Phenom.* **3**, 42 (2008).
- [18] V. M. Kenkre and Niraj Kumar, *Proc. Natl. Acad. Sci. USA* **105**, 18752 (2008).
- [19] E. H. Colombo and C. Anteneodo, *J. Theor. Biol.* **446**, 11 (2018).
- [20] R. S. Cantrell, C. Cosner, and W. F. Fagan, *Math. Biosci.* **175**, 31 (2002).
- [21] W. F. Fagan, R. S. Cantrell, and C. Cosner, *Am. Nat.* **153**, 165 (1999).
- [22] Z. M. Volenec and A. P. Dobson, *Conserv. Biol.* **34**, 66 (2020).
- [23] B. A. Wintle, H. Kujala, A. Whitehead, A. Cameron, S. Veloz, A. Kukkala, A. Moilanen, A. Gordon, P. E. Lentini, N. C. R. Cadenhead, and S. A. Bekessy, *Proc. Natl. Acad. Sci. USA* **116**, 909 (2019).
- [24] W. Van Winkle, Jr., D. C. Martin, and M. J. Sebetich, *Ecology* **54**, 205 (1973).
- [25] J. A. Ross, S. F. Matter, and J. Roland, *Landscape Ecol.* **20**, 127 (2005).
- [26] W. F. Fagan, E. Gurarie, S. Bewick, A. Howard, R. S. Cantrell, and C. Cosner, *Am. Nat.* **189**, 474 (2017).
- [27] J. M. Morales, *Am. Nat.* **160**, 531 (2002).
- [28] E. H. Colombo and C. Anteneodo, *Phys. Rev. E* **92**, 022714 (2015).
- [29] M. Bengfort, H. Malchow, and F. M. Hilker, *J. Math. Biol.* **73**, 683 (2016).
- [30] R. S. Cantrell, C. Cosner, and W. F. Fagan, *Am. Nat.* **158**, 368 (2001).
- [31] G. Vaccario, C. Antoine, and J. Talbot, *Phys. Rev. Lett.* **115**, 240601 (2015).
- [32] R. S. Cantrell and C. Cosner, *Theor. Pop. Biol.* **55**, 189 (1999).
- [33] G. A. Maciel and F. Lutscher, *Am. Nat.* **182**, 42 (2013).
- [34] R. Martínez-García, J. M. Calabrese, T. Mueller, K. A. Olson, and C. López, *Phys. Rev. Lett.* **110**, 248106 (2013).
- [35] S. Chatterjee, R. A. da Silveira, and Y. Kafri, *PLoS Comput. Biol.* **7**, e1002283 (2011).
- [36] K. J. Painter, *J. Theor. Biol.* **481**, 162 (2019).
- [37] A. Okubo and S. A. Levin, *Diffusion and Ecological Problems: Modern Perspectives*, Series: Interdisciplinary Applied Mathematics (Springer, New York, 2001), Vol. 14.
- [38] G. Ariel, A. Rabani, S. Benisty, J. D. Partridge, R. M. Harshey, and A. Be'er, *Nat. Commun.* **6**, 8396 (2015).
- [39] J. E. Sosa-Hernández, M. Santillán, and J. Santana-Solano, *Phys. Rev. E* **95**, 032404 (2017).
- [40] G. M. Viswanathan, M. G. E. da Luz, E. P. Raposo, and H. E. Stanley, *The Physics of Foraging: An Introduction to Random Searches and Biological Encounters* (Cambridge University Press, Cambridge, 2011).
- [41] E. Wong and M. Zakai, *Ann. Math. Statist.* **36**, 1560 (1965).
- [42] P. Hänggi and P. Jung, *Adv. Chem. Phys.* **89**, 239 (1995).
- [43] R. L. Stratonovich, *SIAM J. Control* **4**, 362 (1966).
- [44] M. A. F. dos Santos and I. S. Gomez, *J. Stat. Mech.: Theory Exper.* (2018) 123205.
- [45] R. Kazakevičius and J. Ruseckas, *Phys. Rev. E* **94**, 032109 (2016).
- [46] T. Srokowski, *Phys. Rev. E* **80**, 051113 (2009).
- [47] T. Sandev, A. Schulz, H. Kantz, and A. Iomin, *Chaos, Solitons & Fractals* **114**, 551 (2018).
- [48] A. G. Cherstvy, A. V. Chechkin, and R. Metzler, *New J. Phys.* **15**, 083039 (2013).
- [49] E. E. Holmes, M. A. Lewis, J. E. Banks, and R. R. Veit, *Ecology* **75**, 17 (1994).
- [50] P. Hänggi, *Phys. Rev. A* **25**, 1130 (1982).
- [51] K. Itô, *Proc. Imp. Acad.* **20**, 519 (1944).
- [52] Y. L. Klimontovich, *Phys. A (Amsterdam)* **163**, 515 (1990).
- [53] W. Wang, A. G. Cherstvy, X. Liu, and R. Metzler, *Phys. Rev. E* **102**, 012146 (2020).
- [54] N. Leibovich and E. Barkai, *Phys. Rev. E* **99**, 042138 (2019).
- [55] R. Kupferman, G. A. Pavliotis, and A. M. Stuart, *Phys. Rev. E* **70**, 036120 (2004).
- [56] L. Tupikina, *arXiv:2006.11570*.
- [57] E. H. Colombo, *Ecol. Complexity* **39**, 100777 (2019).
- [58] A. P. Allen, B.-L. Li, and E. L. Charnov, *Ecol. Lett.* **4**, 1 (2001).
- [59] A. Godec and R. Metzler, *Sci. Rep.* **6**, 20349 (2016).
- [60] E. J. Carr, J. M. Ryan, and M. J. Simpson, *J. Chem. Phys.* **153**, 074115 (2020).
- [61] D. T. Gillespie, *Annu. Rev. Phys. Chem.* **58**, 35 (2007).
- [62] E. Hernández-García and C. López, *Phys. Rev. E* **70**, 016216 (2004).